

Photochemical Formation of Silver Nanoparticles in Poly(N-vinylpyrrolidone) Film and Direct Metal Photo-patterning by a Mask

ポリビニールピロリドン中の銀ナノ粒子の光化学形成とマスクによる直接的金属光パターニング

Yu Zhang[†], Shizuyasu Ochiai^{††}, Kenzo Kojima^{††}, Yoshiyuki Uchida^{†††}, Asao Ohashi^{††}

張 宇、落合鎮康、小嶋憲三、内田悦行、大橋朝夫

Abstract: Silver nanoparticle-poly (N-vinylpyrrolidone) composite films (called nano-Ag/PVP) were prepared by Ag⁺ doped PVP thin films irradiated ultraviolet light. The Ag particles in the films exhibited typical fcc (face-centered-cubic) structural X-ray diffraction peaks with broadened nanoparticle linewidth characteristics where the size of Ag nanoparticle is estimated to be approx. 25 nm. Coordination bonding formation between PVP carbonyl oxygen and silver atoms on nanoparticle surfaces (>C=O--Ag) was also demonstrated by using an FTIR spectrum measurement. The photo-generation processes of nano-Ag/PVP composite films with different Ag⁺ doping concentration were investigated by using UV-vis absorption spectroscopy. A photo-reduction growth mechanism of Ag nanoparticles in PVP films is presented, including both initial slow induction periods, to form small Ag particles and subsequent rapid growth stage of Ag particles. Finally, direct metal photo-patterning of PVP thin films was realized using 254nm light irradiation of Ag⁺ doped PVP thin films covered with a mask. So far, silver patterned arrays with a period of 12.5μm (5μm spacing) can be achieved.

1. Introduction

Fabrication of composite systems of metal nanoparticles in polymer films is of considerable interest at present. These materials exhibit novel combinations of particle and polymer properties that are attractive for applications in linear and nonlinear optics^{1,2)}, photo-imaging and patterning³⁻⁵⁾, manufacture of conductive film circuits⁶⁾, magnetic devices⁶⁾, and sensor fabrication⁷⁾, etc. The light-sensitive nature of metal ions such as Ag⁺ and Au³⁺ ions is well known, therefore, one expects to develop light-sensitive ion doped polymer films in order to realize direct metal photo-patterning by a simple mask method combined with UV-light irradiation. This strategy is a photo-resist free approach thus is simple and low-cost, which is different from conventional photolithography techniques

limited by the high costs due to the complex fabrication procedures for resist coating, etching processes, high-energy consumption, and numerous lithographic steps. To date, some light-sensitive ion doped polymer systems and their photo-reduction to form metal nanoparticles-polymer composite films, as well as photo-patterning, have been investigated³⁻⁵⁾, while scientists are seeking various new systems. Mills *et al.* have reported the photochemical formation of Ag nanoparticles in films made from blends of poly (vinyl alcohol), PVA, and poly(acrylic acid), PAA, where the photo-reduction of Ag⁺ ions was initiated by excited polymer⁸⁾. Photosensitive polymer of SPEEK (sulfonated poly-(ether-ether) ketone) with benzophenone groups was also introduced into an Ag⁺ ion doped PVA system as a photo-initiator to reduce Ag⁺ ions, and 40 μm wide Ag line arrays were superimposed on the film surface using a mask combined with UV irradiation⁴⁾.

Poly (N-vinylpyrrolidone), PVP, has high solubility in a wide range of solvents and superb film forming capability, as well as a good stabilizer for metal colloids in solution which has been extensively applied to various colloidal preparations⁹⁻¹⁰⁾. PVP contains a functional group of >C=O which adsorbs 254 nm light. It has been demonstrated that the excited species of >C=O* can reduce Ag⁺ to Ag in aqueous

[†] Key Laboratory of Molecular and Biomolecular Electronics, Ministry of Education, Southeast University (Nanjing in CHINA N)

^{††} Department of Electrical Engineering, Aichi Institute of Technology (Toyota)

^{†††} Department of Information Network Engineering, Aichi Institute of Technology (Toyota)

solution containing PVP with high concentration⁹⁾ at UV irradiation, yet detailed photo-reduction mechanisms were not presented. Polymer electrolytes containing silver salts are currently under intensive investigation because of their potential application in facilitated transport membranes¹¹⁾. PVP is often used as a polymer carrier in the preparation of silver salt-polymer electrolytes, while the high solubility of Ag^+ ions in PVP has been demonstrated due to strong interaction between Ag^+ ions and polar groups of $>\text{C}=\text{O}$ on polymer chains¹²⁻¹³⁾. In this work, Ag^+ doped PVP thin films were used to prepare Silver nanoparticle-PVP (nano-Ag/PVP) composite films using an ultraviolet light-induced photochemical reaction, while the photo-generation procedure of Ag nanoparticles in PVP films was studied by UV-vis absorption spectroscopy. Direct silver patterning polymer thin films were also realized using a simple mask method combined with UV-light irradiation.

2. Experimental Section

2.1 Chemicals

Silver nitrate, AgNO_3 (99.9%) was used as precursor of Ag nanoparticles. Poly (N-vinylpyrrolidone) (PVPK30, MW40 000) was purchased from Wako Pure Chemical Industries, Ltd. Ethanol (EtOH, 99.5%) (Amakasu) was used as solvents. All of the chemicals were used as received from the suppliers.

2.2 Preparation of Nano-Ag/PVP Composite Films and Their Photo-patterning

First, precursor solutions of PVP (9 mM, calculated per polymer units) in ethanol containing AgNO_3 with different concentrations (2.5, 5, and 10 mM) were prepared ($R=[\text{Ag}^+]/[\text{PVP}]=0.28, 0.56, 1.11$, respectively). A 50 μL precursor solution was cast directly onto a cleaned glass microscope cover slip. The formed Ag^+ doped PVP films were then dried at room temperature for 15 min followed by UV-irradiation in the ventilator at different times according to UV-vis absorption variation. Then yellow Ag nanoparticle composite films were obtained and marked as Samples a, b, and c, respectively. The UV lamp used was Toshiba GL20-A 20 W low-pressure mercury lamp with a main irradiation wavelength of 254 nm. The glass microscope cover slip substrates were cleaned for 15 min. in a freshly prepared 1:3 mixture of 30% H_2O_2 and 98% H_2SO_4 (piranha solution) then washed with a large amount of deionized water and ethanol before polymer films were deposited. Silver patterning polymer films were obtained using UV-irradiation of formed Ag^+ doped PVP films covered by a mask where transmission electron microscopy (TEM) copper grids with different hole sizes of 200, 400 and 2000 mesh were used as a mask.

2.3 Characterization Techniques

UV-vis spectra were recorded using a UV-2450 UV-visible spectrophotometer (Shimadzu). FTIR (Fourier transform infrared spectroscopy) measurements were performed on a FTIR-8400S spectrophotometer (Shimadzu). X-ray diffraction (XRD) measurements were performed on a Voyager 1000 X-ray diffractometer with $\text{Cu K}\alpha$ radiation ($\lambda=1.5406 \text{ \AA}$) operated at 40 kV and 40 mA. Silver photo-patterning polymer films were observed using transmission optical microscopy (Olympus BX 50) with a DP 11 digital camera (2.5 M pixels).

3. Results and Discussion

Figure 1 shows an X-ray diffraction pattern of nano-Ag/PVP composite films obtained from the precursor solution with an AgNO_3 concentration of 10 mM. The characteristic diffraction peaks of (111), (200), (220), and (311) indicate fcc structural silver. The broadened diffraction peaks can be observed,

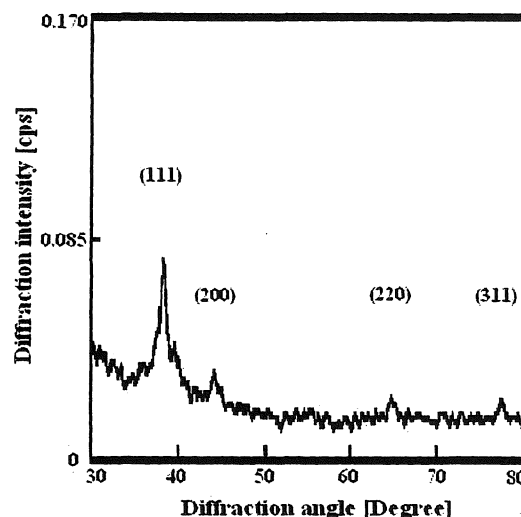


Fig. 1 XRD pattern of nano-Ag/PVP composite film (Sample c).

which are characteristic of nanoparticles. The average crystallite diameter (ACD) of Ag nanoparticles was determined using the XRD linewidth of the (111) peak using Scherrer's Formula¹⁴⁾, with the calculated result being approx. 25 nm.

FTIR spectroscopy was used to study the interaction between silver nanoparticles and polar groups on PVP chains. Figure 2 presents FTIR spectrum of nano-Ag/PVP composite films obtained from the precursor solution with AgNO_3 concentration of 10 mM.

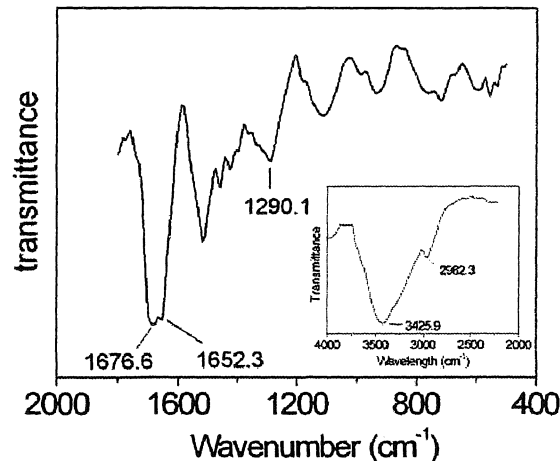


Fig. 2 FTIR spectrum of nano-Ag/PVP composite film (Sample c). Inset shows the spectrum of sample (c) in range of 2000-4000 cm^{-1} .

It is found that carbonyl groups exhibit a broad and splitting absorption band at 1676.6 and 1652.3 cm^{-1} . The former band belongs to free carbonyl groups, while the latter can be attributed to a new carbonyl stretching band which shifts to the lower frequency due to carbonyl groups bound to the surface of Ag nanoparticles through the coordination bonding of $>\text{C}=\text{O}-\text{Ag}$. This result is consistent with the previously reported results for the interaction of Ag^+ ions and PVP¹²⁾. The absorption band at approx. 1290.1 is attributed to C-N stretching vibration. The inset in Figure 2 also shows a broad absorption band at 3425.9 cm^{-1} , caused by the stretching vibration of H_2O adsorbed on PVP chains. The absorption band at 2962.3

Photochemical Formation of Silver Nanoparticles in PVP Film and Direct Metal Photo-patterning by a Mask

cm^{-1} can be attributed to groups of $-\text{CH}_2-$ and $-\text{CH}-$. Silver particles reduced to nanometer dimensions exhibit unique optical properties in the visible spectral range due to the excitation of collective oscillations of conducting electrons known as plasmon resonances or surface plasma¹⁵. UV-vis absorption spectra have been shown to be quite sensitive to the size, shape, and the surrounding dielectric environment of silver nanoparticles thus to their formation processes in solution or films¹⁶⁻¹⁷. Figure 3 shows UV-vis spectral evolutions during the formation of nano-Ag/PVP composite films obtained from the precursor solutions with different AgNO_3 concentrations of 2.5, 5, and 10 mM marked as Samples a, b, and c, respectively.

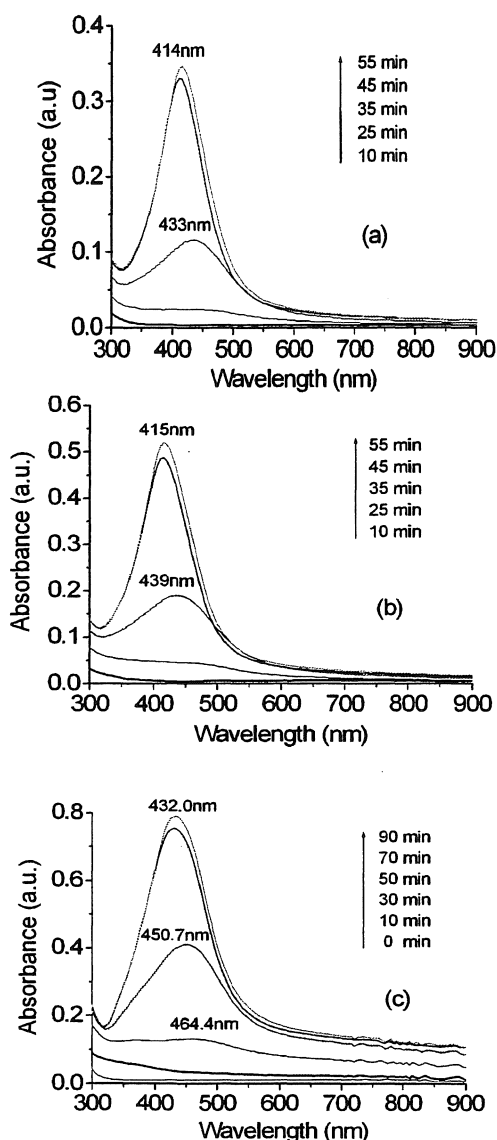


Fig. 3 UV-vis spectral evolution during nano-Ag/PVP composite film formation from precursor solutions with different AgNO_3 concentrations: (a) 2.5mM; (b) 5mM; (c) 10mM.

The films were irradiated with 254 nm UV light. The irradiation time is indicated in the Figure for each spectrum. The absorption spectra of Ag particles in PVP films continuously develop with time until they reach a stable state when all the silver ions have been reduced at 254 nm light irradiation. An obvious absorption band blue-shift and

narrowing for all three Samples can be observed while the shapes of the absorption band ultimately obtained are almost symmetrical, suggesting the nanoparticles are well dispersed in PVP films and sphere-shaped as the aggregation of nanoparticles leads to red-shifted and broadened surface plasmon absorptions¹⁸, while the anisotropic silver nanoparticles result in splitting into multiple bands¹⁶.

Table 1 provides the optical parameters of silver nanoparticles in PVP films obtained from the final absorption spectrum in Figure 3 a, b, and c, including the maximum absorption wavelength of λ_{max} , the maximum absorbance, and the full bandwidth at half-maximum (FWHM).

Table 1. Optical parameters of silver nanoparticles in PVP films obtained from final absorption spectrum of Sample a, b and c in Figures 3

Sample Name	Sample a	Sample b	Sample c
Ag^+ Concentration in Solutions (mM)	2.5	5	10
Ag^+ Amount in Films ($\times 10^{-7}$ mol/ cm^2)	0.26	0.52	1.03
λ_{max} (nm)	414	415	432
Adsorbance at λ_{max}	0.35	0.52	0.79
FWHM (nm)	92	96	120

The maximum absorbance can be said to enhance linearly with increasing Ag^+ ion doping concentration in PVP films where the amount of PVP is constant. Only slight increases are seen for Samples a and b, while strong enhancements take place for Sample c compared with Samples a and b for λ_{max} and FWHM. Huang *et al.* reported the photochemical formation of Ag nanoparticles in aqueous solution in the presence of PVP and indicated that the variation of Ag^+ ion concentration only slightly affected the size and size distribution of Ag nanoparticles in solution⁹. Thus we infer that their behavior is similar to the solution phase formation of Ag nanoparticles for Samples a and b with low Ag^+ ion concentration. This is in agreement with the high solubility of Ag^+ ions in PVP reported by Kang *et al.*¹²⁻¹³. However, ion pairs start to form followed by higher-order ionic aggregates¹² at silver concentration above 1:1 relative to carbonyl oxygen. For Sample c, $R=[\text{Ag}^+]/[>\text{C}=\text{O}]=1.11$. Thus we conclude that the high concentration of Ag^+ ions for Sample c leads to the formation of Ag nanoparticles with large and broad distribution responsible for both the large λ_{max} and FWHM. It has been demonstrated that the absorption peak shifts toward longer wavelengths as particles become larger⁹. In Huang's studies, silver colloids with an average size of 15.2 to 22.4 nm were obtained, with the corresponding UV-vis absorption peaks from 404 to 418 nm⁹. It is reasonable to estimate sizes for our Ag nanoparticles in PVP films at a range from 15 to 30 nm according UV-vis absorption spectra that agree with the sizes calculated from XDR by considering the effect of surrounding medium refractive indices¹⁰ (PVP film has higher refractive indices than water solutions, resulting in a red-shift of the absorption band). Theoretical calculations have revealed that the dipolar plasmon absorption is dominant in this size range^{9,16} thus the symmetric absorption peaks for the films ultimately obtained can be observed.

A marked intensity increase and absorption band blue-shift can be observed clearly in Figure 3 for all three Samples at UV irradiation. It may be difficult to decipher the blue-shifts as the gradual growth of Ag particles should lead to size increases, thus to the red-shift of the absorption band according to the above discussion. Theoretical investigations have indicated that the oscillation frequency of surface plasma in metal nanoparticles not only depends on effective electron mass, the

size and shape of the charge distribution, but is also affected by the density of electrons¹⁶⁾. The wavelength of the absorption maximum is proportional to the reciprocal square root of the metal electron density²⁰⁾. It has been demonstrated by Henglein *et al.* that the surface Ag^+ ion absorptions can greatly reduce the density of free electrons in Ag nanoparticles dispersed in aqueous solution, thus result in the absorption peak red-shift by multiple nanometers²⁰⁾. Compared with the results of Huang's study, the effect of size increases on λ_{max} is much smaller than that of surface ion absorption. As a result, the observed blue-shift in Figure 3 can be explained by the consumption of Ag^+ ions in the photo-reduction reaction, which causes a decrease in the amount of Ag^+ ions adsorbed on particle surfaces, although Ag particles gradually increase. The Ag^+ ion consumption most likely takes place from the photo-reduction of the adsorbed Ag^+ ions on particle surfaces. The following section will discuss the photo-reduction of Ag^+ ions to form Ag nanoparticles in PVP films.

Figure 4 shows the absorption intensity at λ_{max} as a function of the photo-reduction reaction time for Samples a, b and c shown in Figure 3.

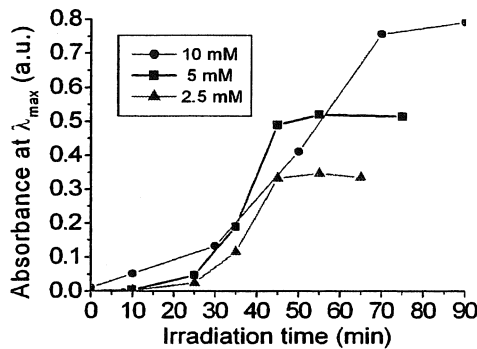
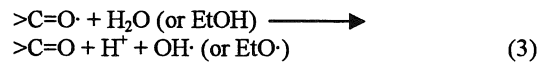
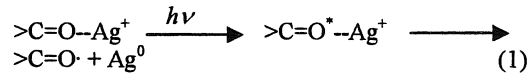


Fig. 4 Absorption intensity at λ_{max} as a function of photoreduction reaction time for samples (a), (b), and (c) shown in Figure 1.

We use the change of absorption intensity to reflect the photo-reduction reaction of Ag^+ ions, although the absorption intensity is relative not only to the particle concentration formed, but also to the particle size, aggregate state, etc.. There are two distinct reaction stages before the final stable state. The first stage is from the beginning of the reaction to the time at 25-30 min., in which the formation rate of Ag particles is very slow and a wide absorption region starting from 300 nm is observed without the characteristic absorption peak of Ag nanoparticles. Ag clusters of a few atoms of Ag_n ($n=1-3, 4-7,$ and $8-12$) were characterized with UV absorption bands at 292, 325, and 370-380 nm, respectively in the earlier γ -irradiation study of aqueous silver nitrate solution²¹⁾. Thus the wide absorption region observed in the present study can be reasonably attributed to the existence of Ag clusters with different n values, as well as small Ag particles. In the second stage, the formation rate of Ag particles is dramatically accelerated while the characteristic absorption peak of Ag nanoparticles appears and blue-shifts occur with the consumption of Ag^+ ions.

PVP contains a functional group of $>\text{C}=\text{O}$ which adsorbs 254 nm light more strongly than Ag^+ ions in our experimental conditions and has strong interaction with Ag^+ ions or Ag nanoparticles through the coordination bonding as shown by the FTIR spectrum. The formation of the coordination bonding induces a fractional electron transfer from the carbonyl group to silver. According to Henglein's work, this effect induces a

displacement of the metal Fermi level toward the more negative potentials²⁰⁾. Simultaneously, the carbonyl group redox potential increases and becomes easier to photo-oxidize. The excited species of $>\text{C}=\text{O}^*$ can reduce Ag^+ ions to Ag atom as a result at 254 nm light irradiation. Subsequent agglomeration of Ag atoms occurs to form Ag clusters and small Ag particles. Possible reaction mechanisms are as follows.



The free radicals of $>\text{C}=\text{O}^\cdot$ formed are reverted to $>\text{C}=\text{O}$ by the reaction with water or ethanol adsorbed in PVP films. Similar free radical reaction was also shown in the previous reports on the photo-reduction of Ag^+ ions in surface-modified polyimide layers where the carboxyl radicals of $-\text{CO}_2^\cdot$ undergo a similar reaction⁹⁾. Henglein *et al.* performed a detailed investigation of the photo-reduction of Ag^+ ions in aqueous solution in the presence of acetone and 2-propanol, where the photo-reduction was initiated by acetone ketyl radicals with a low rate of reaction²⁰⁾. Similar low reaction rates should also appear in our reaction system for Eq. 1. This slow reaction period can be called an induction period for silver reduction, corresponding to the first stage shown in Figure 3.

With the gradual formation of the small Ag particles, a second reduction process occurs, in which Ag^+ ions are reduced on the surface of the Ag particles, as Ag nanoparticles can act as an electron storage and transfer medium. It has been observed by Henglein²⁰⁾ and Brus²²⁾ *et al.* that there is a displacement of plasmon resonance after electron injection inside Ag nanoparticles, and an increase of the chemical reactivity on particle surfaces. Thus the excited species of $>\text{C}=\text{O}^*$ first transfer an electron to Ag particles, then the Ag^+ ions adsorbed on its surfaces are reduced by stored electrons in the second stage, resulting in the gradual growth of Ag particles with a faster rate. The electron transfer procedures are illustrated in Figure 5.

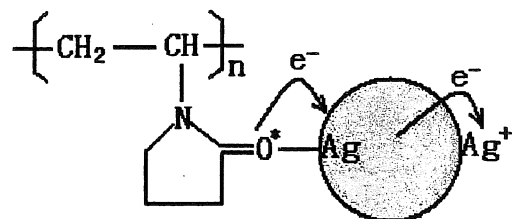


Fig. 5 Electron transfer process from excited species of $>\text{C}=\text{O}^*$ to Ag^+ ions adsorbed on Ag nanoparticle surfaces.

Similarly, both the slow induction period and rapid particle growth stage could be observed for all three samples with different initial Ag^+ concentrations (Figure 4). However, the final absorbance in the two stages increases with the initial Ag^+ concentrations in PVP films. The increase of the initial Ag^+ concentrations results in forming more coordination bonding of $>\text{C}=\text{O}-\text{Ag}^+$ in the induction period, which is helpful to facilitate the photo-reduction of Ag^+ ions. Yet in the second stage, the largest rate of increase in absorbance may be observed for Sample b in comparison to Sample a and c, suggesting that the Ag particle formation rate is dependent not only on the initial Ag^+ concentration but also on the relative

Photochemical Formation of Silver Nanoparticles in PVP Film and Direct Metal Photo-patterning by a Mask

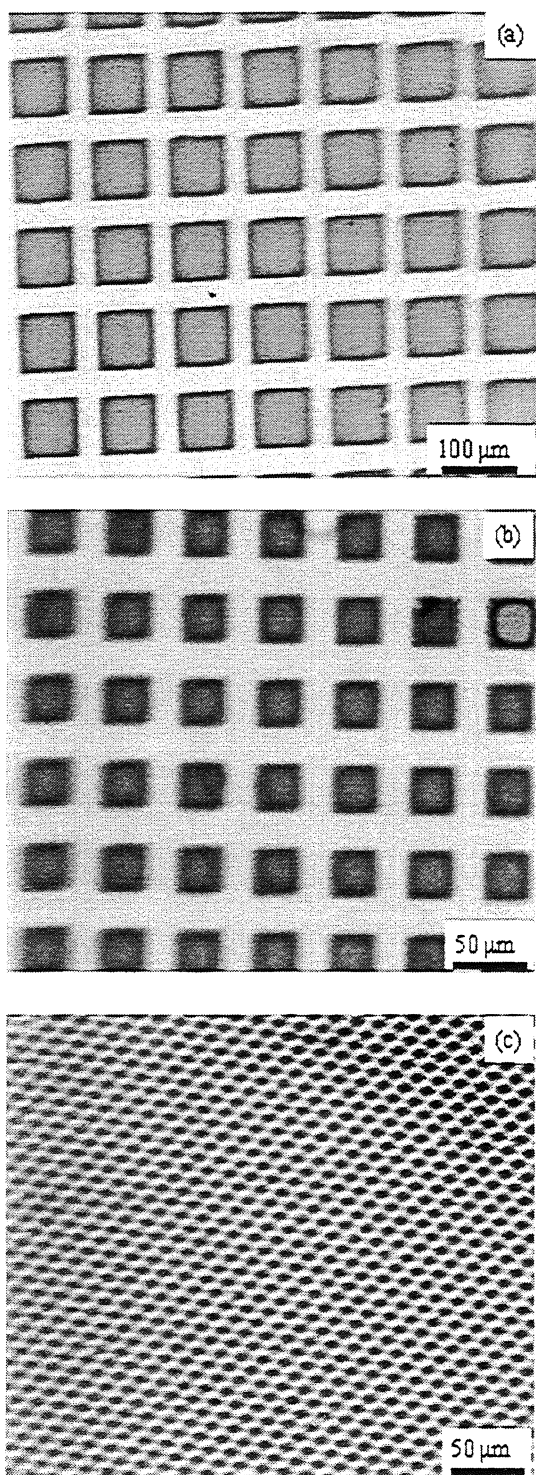


Fig. 6 Transmission optical microscopy images of silver patterned polymer thin films formed from UV irradiation of Ag^+ ion doped PVP films (Ion concentration: 1.03×10^{-7} mol/cm²) for 90 min. Using a copper grid as mask with different hole sizes: (a) 200 mesh, (b) 400 mesh, (c) 2000 mesh.

amount of PVP to Ag^+ . The relatively high PVP concentration may be useful for electron transfer forming PVP to Ag particles.

PVP has good solubility in water and ethanol. However, the nano-Ag/PVP composite films obtained exhibit very good

stability for water and ethanol. No changes in absorption spectra were observed when immersing the films into water and ethanol for 3 hours. This can be reasonably attributed to the cross-linking interaction between PVP and Ag nanoparticles.

An application for direct metal photo-patterning polymer thin films has been realized using Ag^+ ion doped PVP thin films and a TEM copper grid as a mask. Figure 6 shows the obtained silver patterned PVP thin films with different periods. Pattern dimensions are in strong agreement with the photomask used. An array period of 12.5 μm and resolution of 5 μm array spacing are achieved as observed in Figure 6 c. The ultimate resolution of this patterning method remains unknown. Further study is currently being conducted.

4. Conclusions

Nano-Ag/PVP composite films were fabricated using ultraviolet light irradiation of Ag^+ doped PVP thin films obtained from an AgNO_3 -PVP-ethanol mixing solution with a simple casting method. This is a simple photo-reduction system to fabricate silver/polymer composite films, where PVP acts simultaneously as film matrix and photo-reductant. The Ag nanoparticles in the PVP films have a typical fcc structure characterized by X-ray diffraction. The coordination bonding formation between PVP carbonyl oxygen and silver atom on nanoparticle surfaces ($>\text{C}=\text{O}-\text{Ag}$) was also demonstrated by FTIR spectrum measurement. The photo-generation processes of nano-Ag/PVP composite films with different Ag^+ doping concentrations were investigated using UV-vis absorption spectroscopy. A photo-reduction growth mechanism of Ag nanoparticles in PVP films was presented, including both initial slow induction periods to form small Ag particles and the subsequent rapid growth stage of Ag particles. One application is direct metal photo-patterning of PVP thin films realized using 254nm light irradiation of Ag^+ doped PVP thin films covered with a mask. So far, silver patterned arrays with a period of 12.5 μm (5 μm spacing) can be formed.

Acknowledgments

The present work was conducted as part of the research project "Materials for the 21st Century-Materials Development for Environment, Energy, and Information" (for fiscal year 2002-2006) supported by the Ministry of Education, Culture, Sports, Science, and Technology.

- (1) A. Heilmann: *Polymer Films with Embedded Metal Nanoparticles*; Springer Series in Materials Science 52, (Springer Berlin, 2003)
- (2) M. Jose-Yacamán, R. Perez, P. Santiago, M. Benaissa, K. Gonsalves, G. Carlson, *Appl. Phys. Lett.* **69** (1996) 913.
- (3) O. L. A. Monti, J. T. Fourkas, D. J. J. Nesbitt, *Phys. Chem.* **108** (2004) 1604.
- (4) A. S. Korchev, M. J. Bozack, B. L. Slaten, G. J. Mills, *Am. Chem. Soc.* **126** (2004) 10.
- (5) K. Akamatsu, S. Ikeda, H. Nawafune, *Langmuir* **19** (2003) 10366.
- (6) I. W. Park, M. Yoon, Y. M. Kim, Y. Kim, H. Yoon, H. J. Song, V. Volkov, A. Avilov, Y. Park, *J. Solid State Commun.* **126** (2003) 385.
- (7) F. P. Zamborini, M. C. Leopold, J. F. Hicks, P. J. Kulesza, M. A. Malik, R. W. Murray, *J. Am. Chem. Soc.* **124** (2002) 8958.
- (8) G. A. Gaddy, J. L. McClain, E. S. Steilgerwalt, R. Broughton, B. L. Slaten, G. Mills, *J. Cluster Sci.* **12** (2001) 457.

- (9) H. H. Huang, X. P. Ni, G. L. Loy, C. H. Chew, K. L. Tan, F. C. Loh, J. F. Deng, G. Q. Xu, *Langmuir* **12** (1996) 909.
- (10) I. Pastoriza-Santos, L. M. Liz-Marzan, *Langmuir* **18** (2002) 2888. Y. Yoon, J. Won, Y. S. Kang, *Macromolecules* **33** (2000) 3185. (11) J. H. Jin, S. U. Hong, J. Won, Y. S. Kang, *Macromolecules* **33** (2000) 4932.
- (12) S. Choi, J. H. Kim, Y. S. Kang, *Macromolecules* **34** (2001) 9087.
- (13) M. Ma, Y. Zhang, X. B. Li, D. G. Fu, H. Q. Zhang, N. Gu, *Coll. Surf. A*, **224** (2003) 207.
- (14) U. Kreibig, M. Vollmer, *Optical Properties of Metal Clusters*, (Springer, Verlag: Berlin, Heidelberg, 1995)
- (15) K. L. Kelly, E. Coronado, L. L. Zhao, G. C. J. Schatz, *J. Phys. Chem. B* **107** (2003) 668.
- (16) M. Kerker, O. Siiman, D. S. Wang, *J. Phys. Chem.* **88** (1984) 3186.
- (17) J. Zheng, M. S. Stevenson, R. S. Hikida, P. Gregory Van Patten, *J. Phys. Chem. B* **106** (2002) 1252.
- (18) S. M. Heard, F. Grieser, C. G. Barraclough, J. V. Sanders, *J. Colloid Interface Sci.* **93** (1983) 545.
- (19) A. Henglein, *Chem. Mater.* **10** (1998) 444.
- (20) M. Mostafavi, M. O. Delcourt, G. Picq, *Radiat. phys. Chem.* **41** (1993) 453
- (21) M. Maillard, P. Huang, L. Brus, *Nano Lett.* **3** (2003) 1611.

(受理 2006年5月2日)